View metadata, citation and similar papers at core.ac.uk

brought to you by CORE

provided by Digital.CSIC

ARTICLE

Building 1D Lanthanide Chains and non-symmetrical [Ln_2] "Triple-Decker" Clusters Using Salen-type Ligands: Magnetic Cooling and Relaxation Phenomena

Received 00th January 20xx,
Accepted 00th January 20xx

DOI:

Angelos B. Canaj,[a] Milosz Siczek,[b] Marta Otręba,[b] Tadeusz Lis,[b] Giulia Lorusso,[c] Marco Evangelisti[c,*] and Constantinos J. Milios[a,*]

The solvothermal reaction between $Ln(NO_3)_3{\cdot}6H_2O$ (Ln: Gd, Tb and Dy), 2-hydroxy-1-naphthaldehyde , 2-OH-naphth, and ethylenediamine, en, in MeOH in the presence of base, NEt_3, led to the formation of the 1D coordination polymers $[Ln(L)(MeO)(MeOH)_{0.5}]_n{\cdot}MeOH$ (Ln = Gd (**1**·MeOH), Tb(**2**·MeOH), Dy (**3**·MeOH); H_2L= the Schiff-base ligand derived from the condensation of 2-OH-naphth and en), while the similar reaction in excess of NaN_3 yielded 1D coordination polymers $[Ln(L)(N_3)_{0.75}(MeO)_{0.25}(MeOH)]_n$ (Ln = Gd (**4**), Tb (**5**), Dy (**6**)). Finally, upon replacing ethylenediamine with *o*-phenylenediamine, *o*-phen, we managed to isolate the discrete dimers $[Dy_2(L')_3(MeOH)]{\cdot}2MeOH$ (**7**·2MeOH) and $[Gd_2(L')_3(MeOH)]{\cdot}2MeOH$ (**8**·2MeOH) (H_2L' = the Schiff-base ligand from the condensation of 2-OH-naphth and *o*-phen). Polymers **1**-**3** describe one-dimensional chains, containing alternating seven- and eight-coordinate Ln^{III} metal centers, polymers **4**-**6** contain eight-coordinate lanthanide ions, while in both **7** and **8** the two Ln^{III} centers are eight- and seven-coordinate, adopting square antiprismatic and "piano-stool" geometry, respectively. The magnetocaloric properties of the three Gd^{III} analogues were determined from magnetic measurements, yielding the magnetic entropy change $-\Delta S_m$ = 21.8, 23.0 and 16.0 J $kg^{-1}K^{-1}$ at T = 3.0 K on demagnetization 7 T to 0, for **1**, **4** and **8**, respectively. The study of the magnetic properties also revealed that all three Dy^{III} analogues (**3**, **6** and **7**) display out-of-phase signals, therefore suggesting slow magnetic relaxation, while such behaviour was not established in the Tb^{III} analogues.

Introduction

The study of the magnetic properties of lanthanide compounds has witnessed an exponential growth over the last few years; a statement valid for both extended coordination polymers, as well as discrete molecules. Despite the fact that lanthanide compounds attracted the interest of magnetochemists and physicists in the early days of molecular magnetism,[1] it was confined only to a handful of examples, mainly due to the lack of suitable theories and models that could interpret the magnetic behaviour and experimental data of such species, because of the lanthanides' unquenched orbital momentum. Yet, this field received great impulse in 2003 upon the discovery that the mononuclear complexes $(NBu_2)[Pc_2Ln]$ (Pc = dianion of phthalocyanine; Ln = Tb, Dy) could retain their magnetization once magnetized in very low temperatures in the absence of an external magnetic field, and thus function as single molecule magnets (SMMs), with energy barriers for the re-orientation of the magnetization of 330 K and 40 K for the Tb and Dy analogues, respectively.[2] Today, many examples of lanthanide clusters displaying slow relaxation of magnetization have been discovered,[3] while species with extremely high energy barriers, *i.e.* 810 K[4] and 842 K,[5] have been characterized and reported. During the last 6-8 years, molecular complexes containing lanthanides have also attracted much interest since they showed rich magnetocaloric properties and were found to be excellent magnetic refrigerants at cryogenic temperatures.[6] At the basis of magnetic refrigeration is the magnetocaloric effect (MCE), *i.e.*, the changes of magnetic entropy and adiabatic temperature, following a change in the applied magnetic field. Gadolinium is often present because its orbital angular momentum is zero and it has the largest entropy per single ion, which ultimately favor a large MCE.[7] Weak superexchange interactions, as commonly found in molecular complexes based on gadolinium, promote a fast field-dependence of the MCE because of the many low-lying excited states.[7,8]

Given the complexity of the lanthanides-containing reaction schemes, it is important for coordination chemists to gain some "control" over the products of such systems, as a means of synthesizing related species, and eventually comprehend all factors that affect the magnetic properties of such compounds. Of course, given the degree of the serendipitous-assembly principle governing such systems,[9] such a task is not trivial at all.

In this work we present our efforts towards synthesizing related lanthanide species; we have managed to isolate and characterize two families of related 1-D coordination polymers, $[Ln(L)(MeO)(MeOH)_{0.5}]_n{\cdot}MeOH$ (Ln = Gd (**1**·MeOH), Tb (**2**·MeOH), Dy (**3**·MeOH); L = the Schiff-base ligand from the condensation of 2-OH-naphth and en, Scheme 1) and $[Ln(L)(N_3)_{0.75}(MeO)_{0.25}(MeOH)]_n$ (Ln = Gd (**4**), Tb (**5**), Dy (**6**); L =

[a] Department Of Chemistry, University of Crete, Voutes 71003, Herakleion, Greece. Fax: +30-2810-545001; Tel: +30-2810-545099; E-mail: komil@uoc.gr.
[b] Faculty of Chemistry, University of Wroclaw, Joliot-Curie 14, Wroclaw 50-383, Poland.
[c] Instituto de Ciencia de Materiales de Aragón (ICMA), CSIC – Universidad de Zaragoza, 50009 Zaragoza, Spain.

† Footnotes relating to the title and/or authors should appear here.
Electronic Supplementary Information (ESI) available: [details of any supplementary information available should be included here]. See DOI: 10.1039/x0xx00000x

Please do not adjust margins

Please do not adjust margins

the Schiff-base ligand from the condensation of 2-OH-naphth and en), and we also succeeded in isolating the discrete dinuclear units $[Dy_2(L')_3(MeOH)]\cdot 2MeOH$ (**7**·2MeOH) and $[Gd_2(L')_3(MeOH)]\cdot 2MeOH$ (**8**·2MeOH) (L' = the Schiff-base ligand from the condensation of 2-OH-naphth and *o*-phen, Scheme 1).

Experimental Section

Materials and physical measurements

All manipulations were performed under aerobic conditions, using materials as received. Elemental analyses (C, H, N) were performed by the University of Ioannina microanalysis service. Variable-temperature, solid-state direct (dc) and alternating (ac) current magnetic susceptibility data, as well as isothermal magnetization down to 2.0 K were collected on a Quantum Design MPMS-XL SQUID magnetometer equipped with a 5 T DC magnet at the University of Zaragoza. Diamagnetic corrections were applied to the observed paramagnetic susceptibilities using Pascal's constants. Powder XRD measurements were collected on freshly prepared samples of **2**, **3, 4** and **8** on a PANalytical X'Pert Pro MPD diffractometer at the University of Crete.

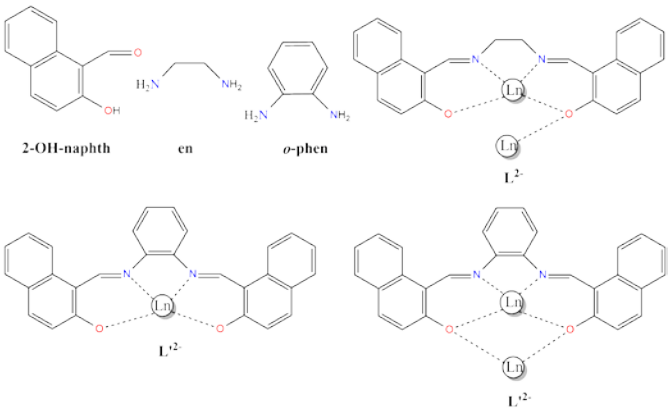

Scheme 1 The structures of all ligands discussed in the text, and their coordination modes in **1-8**.

Syntheses

General synthetic strategy applicable to **1**-**3***:*

In a typical procedure, $Ln(NO_3)_3\cdot 6H_2O$ (0.33 mmol), 2-OH-naphth (113 mg, 0.66 mmol), en (0.33 mmol) and NEt_3 (2.0 mmol) were added in MeOH (10 ml total volume) and transferred to a Teflon-lined autoclave and kept at 120 °C for 12 hours. After slow cooling to room temperature, light yellow-brown needle crystals of $[Ln(L)(MeO)(MeOH)_{0.5}]_n\cdot MeOH$ were obtained in ~25 % yield and collected by filtration, washed with Et_2O and dried in air. Elemental Anal. calcd (found) for **1**: C 53.66 (53.52), H 4.06 (4.29), N 4.91 (5.01); **2**: C 53.51 (53.37), H 4.05 (4.30), N 4.90 (5.04); **3**: C 53.18 (53.31), H 4.03 (3.78), N 4.86 (4.71)

General synthetic strategy applicable to **4**-**6**:

In an analogous procedure with that followed for **1-3**, in the presence of NaN_3 (33 mg, 0.5 mmol) light yellow-brown needle crystals of $[Ln(L)(N_3)_{0.75}(MeO)_{0.25}(MeOH)]_n$ were obtained in ~25% yield and collected by filtration, washed with Et_2O and dried in air. Elemental Anal. calcd (found) for **4**: C 50.97 (51.11), H 3.85 (3.61), N 10.00 (10.15); **5**: C 50.83 (50.95), H 3.84 (3.60), N 9.98 (9.85); **6**: C 50.53 (50.62), H 3.82 (3.59), N 9.90 (9.75).

General synthetic strategy applicable to **7**-**8**:

$Ln(NO_3)_3\cdot 6H_2O$ (0.33 mmol), 2-OH-naphth (113 mg, 0.66 mmol), *o*-phen (0.036 mg, 0.33 mmol) and NEt_3 (2.0 mmol) were added in MeOH (10 ml total volume) and transferred to a Teflon-lined autoclave and kept at 120 °C for 12 hours. After slow cooling to room temperature, orange needle crystals of $[Ln_2(L)_3(MeOH)]\cdot 2MeOH$ were obtained in ~20% yield and collected by filtration, washed with Et_2O and dried in air. Elemental Anal. calcd (found) for **7**·MeOH: C 63.31 (63.18), H 3.77 (4.01), N 5.15 (5.29); Anal. calcd (found) for **8**·MeOH: C 63.72 (63.59), H 3.79 (4.03), N 5.18 (5.33).

X-Ray Crystallography

Diffraction data for **1**·MeOH, **6** and **7**·2MeOH were collected at 100 K on an Xcalibur RUBY and KUMA diffractometer. All structures were solved by direct methods and refined by full-matrix least-squares technique on F2 with SHELXL.[10] In **1**·MeOH all non-hydrogen were found directly form the solution of the structure. In further stages of refinement occupancy of coordinated methanol molecule was refined freely and finally fixed at 0.5. Therefore Gd atom is alternately seven- (MeOH not coordinated) or eight-coordinate (MeOH coordinated). In **6**·2MeOH, from E-map position of Dy and all non-H atoms from L' ligand were found. After refinement additional maxima appeared. These peaks were interpreted as statistical disordered azide and methoxy groups which are in the same position. In the final refinement, disorder was modelled with the occupancy of 0.75 for N-atoms from azide and 0.25 for methoxy group. Atoms N1 and O2 and also N2 and C2 were modelled using EADP instruction. The non-hydrogen atoms, except disordered atoms from azide (N1, N2) and methoxy (O2, C2), were refined anisotropically. Hydrogen atoms were placed in calculated positions and refined using a riding model.[10] Data collection parameters and structures solution and refinement details are listed in Table S1. Full details can be found in the CIF files: 1494777-1494779.

Results and Discussion

Syntheses

The reaction between $Ln(NO_3)_3\cdot 6H_2O$ (Ln = Gd, Tb, Dy), 2-hydroxy-1-naphthaldehyde, 2-OH-naphth, and ethylenediamine, en, in MeOH under solvothermal conditions, in the presence of base, NEt_3, led to the formation and isolation of three new 1D coordination polymers of the general formulae $[Ln(L)(MeO)(MeOH)]_n\cdot MeOH$ (Ln = Gd (**1**·MeOH), Tb (**2**·MeOH), Dy (**3**·MeOH); L = the Schiff-base ligand from the condensation of 2-OH-naphth and en) according to eqn. (1):

$$n\ Ln(NO_3)_3\cdot 6H_2O + 2n\ \text{2-OH-naphth} + n\ \text{en} \xrightarrow{\text{MeOH, base}}$$

Please do not adjust margins

$$[Ln(L)(MeO)(MeOH)_{0.5}]_n\cdot MeOH + 3n\ HNO_3 + 6n\ H_2O \quad (1)$$
(Ln = Gd (**1**·MeOH), Tb (**2**·MeOH), Dy (**3**·MeOH))

The reaction was carried out in a 1:2:1 Ln:2-OH-naphth:en ratio, as a means of favoring the formation of the salen-type ligand H_2L. Furthermore, increasing the metal:ligands' ratio did not lead to different crystalline products, as verified by means of pXRD and IR spectra comparison; on the contrary it led to a decrease of the reactions' yield. In addition, repeating the reaction under normal "bench" laboratory conditions did not lead to the formation of any material, crystalline or powder, thus proving the need for heat/pressure.

Given the presence of the bridging methoxide in the structures of **1**-**3** (*vide infra*) the next step for us was to replace it with an azide anion, N_3^-, as a means of potentially propagating ferromagnetic interactions between the metallic centres (*vide infra*).[11] Therefore, we repeated the reaction in the presence of excess NaN_3, and we managed to isolate the three "azide" analogues of the general formulae $[Ln(L)(N_3)_{0.75}(MeO)_{0.25}(MeOH)]_n$ (Ln = Gd (**4**), Tb (**5**), Dy (**6**)), according to eqn. (2):

$$n\ Ln(NO_3)_3\cdot 6H_2O + 2n\ 2\text{-OH-naphth} + n\ en + n\ NaN_3 \xrightarrow[base]{MeOH,}$$

$$[Ln(L)(N_3)_{0.75}(MeO)_{0.25}(MeOH)]_n + 2n\ HNO_3 + 1n\ NaNO_3 + 6n\ H_2O \quad (2)$$
(Ln= Gd (**4**), Tb (**5**), Dy (**6**))

Finally, the last goal was to block the polymerization process, and for that reason we used *o*-phenylenediamine, *o*-phen, which carries a rigid aromatic "linker" between the two amine groups, rather than a "flexible" ethylene group as in the case of ethylenediamine. Indeed, we managed to stop the polymerization process, and we were able to isolate the Dy and Gd dimers $[Dy_2(L')_3(MeOH)]\cdot 2MeOH$ (**7**) and $[Gd_2(L')_3(MeOH)]\cdot 2MeOH$ (**8**), according to eqn. (3):

$$2Ln(NO_3)_3\cdot 6H_2O + 3\ 2\text{-OH-naphth} + 3\ o\text{-phen} \xrightarrow{MeOH,\ base}$$

$$[Ln_2(L')_3(MeO)(MeOH)] + 6\ HNO_3 + 12\ H_2O \quad (3)$$
(Ln= Dy (**7**), Gd (**8**))

We were able to obtain large single crystals suitable for X-ray single-crystal crystallography for all eight complexes. Yet, since all complexes displayed both similar pXRD diagrams (Figs. S1, S2) and IR spectra (Fig. S3), we chose to solve only the representative crystal structures of **1**·MeOH, **6** and **7**·2MeOH. Despite our attempts to isolate the Tb dimeric analogue, all our efforts proved fruitless.

Description of structures

The molecular structure of $[Gd(L)(MeO)(MeOH)_{0.5}]_n\cdot MeOH$ (**1**·MeOH) is presented in Figure 1, while selected bond distances and angles are given in Table S2. The compound crystallizes in the orthorhombic *Pccn* space group. Its structure consists of alternating [Gd(L)(MeO)(MeOH)] and [Gd(L)(MeO)] units forming 1D chains running perpendicular to the *ab* plane. Each unit is connected to its neighboring units *via* two bridging μ-OCH_3^- and two μ-OR^- groups, with the latter belonging to two salen-type ligands, HL^-. Each ligand, is found in its dianionic form, L^{2-}, adopting a 2.2111 coordination mode (Harris notation[12]), forming three chelate rings around the central lanthanide ion, and further bridging *via* one alkoxide group to a neighboring lanthanide center. The gadolinium centers are seven and eight-coordinate, with the latter ones adopting triangular dodecahedral geometry, as found by a SHAPE[13] analysis (Figure 2). The distance between neighboring Gd centers within the same chain is ~3.95 Å. In the crystal, the chains run parallel to each other, with the closest Gd···Gd distance for metals belonging to neighboring chains being ~8.21 Å, while finally there are no inter-chain H-bonds present (Figure 3). The molecular structure of compound **6** is shown in Figure 4, while selected bond distances and angles are given in Table S3. The molecule crystallizes in the orthorhombic *Pbca* space group, and its structure resembles the structure of **1** with the major difference being the presence of an μ-*end-on* N_3^- group *vs*. the μ-OCH_3^- group present in **1**. Again, each ligand is found in its dianionic form, L^{2-}, adopting a 2.2111 coordination mode, while as in the case of **1**, each lanthanide center is eight-coordinate adopting triangular dodecahedral geometry.

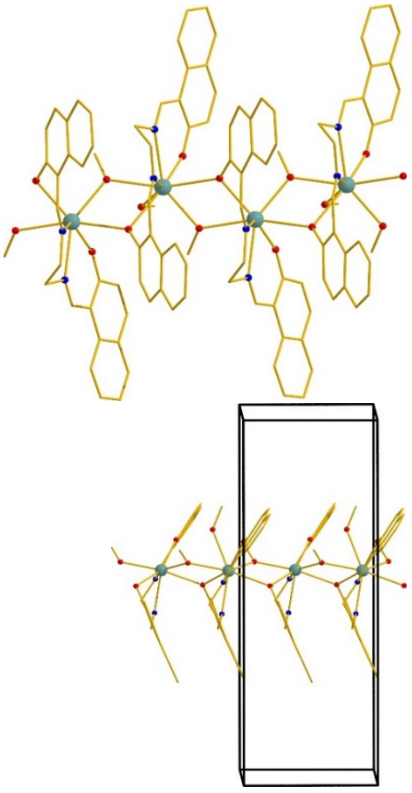

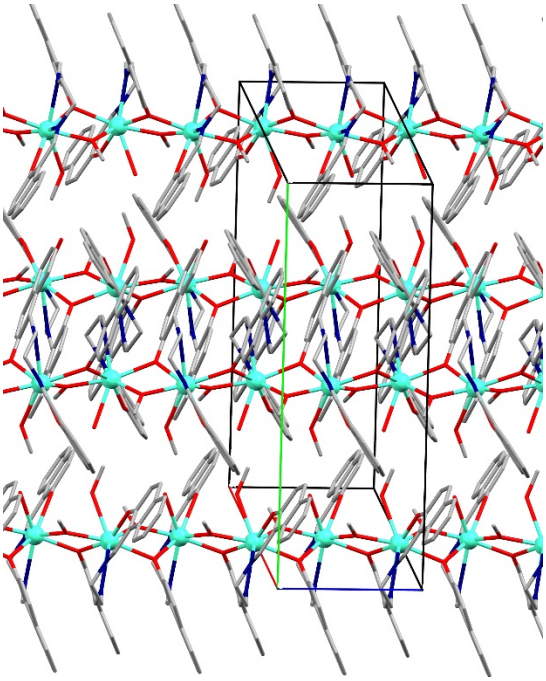

Figure 1 The polymeric structure of **1** looking down *b* (top) and *a* (bottom) axis. Colour code: Gd: green, O: red, N: blue, C: yellow.

Figure 2 The coordination geometry of the eight-coordinate Gd^{III} centers in **1**. Colour code: same as in Figure 3.

The similarity of compounds **1** and **6** is presented in Figure 5; the overlay of the two structures clearly demonstrates that the main difference is indeed the replacement of the methoxide, μ-OCH_3^-, groups in **1** with azide, μ-1,1-N_3^- ligands. In **1** the Ln-$O_{methoxide}$-Ln angle is ~116.8°, while in **6** the Ln-N_{azide}-Ln angle is slightly decreased to ~110.0°.

Figure 3 Crystal packing for **1**.

Figure 4 The molecular structure of **6** looking down *c* axis. Colour code: Dy: green, O: red, N: blue, C: yellow.

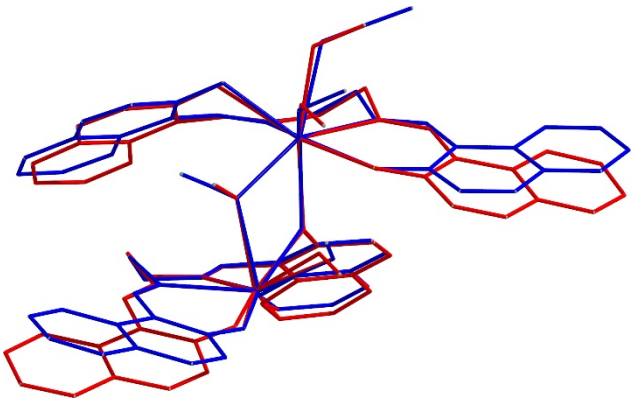

Figure 5 Overlay of the two structures of **1** (red) and **6** (blue).

The crystal structure of complex **7** is shown in Figure 6, while bond distances and angles are given in Table S4. The complex crystallizes in the triclinic *P-1* space group. It consists of the

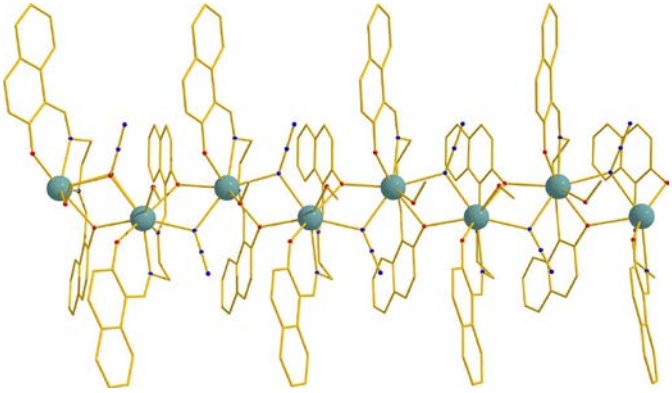

dimeric metallic unit $[Dy_2(\mu\text{-}O_R)_2]$ which is held in position by two alkoxide groups belonging to one doubly deprotonated L^{2-} ligand, with bridging Dy-O_R-Dy angles of 111.45(13)° and 110.83(12)°, and the dysprosium centers separated by 3.872(2) Å. All three ligands, fully deprotonated, adopt two coordination modes: two are found in a strictly chelate 1.1111 fashion, forming three chelates rings around the lanthanide center, while the remaining central ligand is found in a 2.2211 binding fashion. Furthermore, the metal ions are not located in the same plane with the L^{2-} ligands, but are located between neighboring ligands, thus forming a "triple-decker" cluster. The two Dy^{III} centres are seven- and eight-coordinate, with the latter one adopting square antiprismatic geometry, and the former one a distorted "piano-stool" geometry,[14] in which the triangular upper $\{O_3\}$ plane and the lower $\{O_2N_2\}$ plane are converging, deviating from parallel by ~11° (Figure 7). Furthermore, Dy2 is displaced ~1.1 Å out of the mean $\{O_2N_2\}$ plane, and ~1.6 Å from the $\{O_3\}$ plane. Respectively, Dy1 is displaced ~1.3 Å from the upper $\{O_2N_2\}$ face of the square antiprism, and ~1.5 Å from the lower $\{O_2N_2\}$ one.

Figure 6 The molecular structure of **7.** Colour code: Dy: green, O: red, N: blue, C: yellow.

Figure 7 The coordination geometry of Dy1 in cluster **7** (left); the distorted "piano-stool" conformation of Dy2 in **7** (right). Colour code: Dy: green, O: red, N: blue, C: yellow.

In the crystal structure there are three intermolecular H-bonds, between the coordinated MeOH ligand, the two solvate MeOH molecules and one deprotonated alkoxide group bound on Dy1 (Figure 8). Finally, there are no intermolecular H-bonds linking neighboring dimeric units.

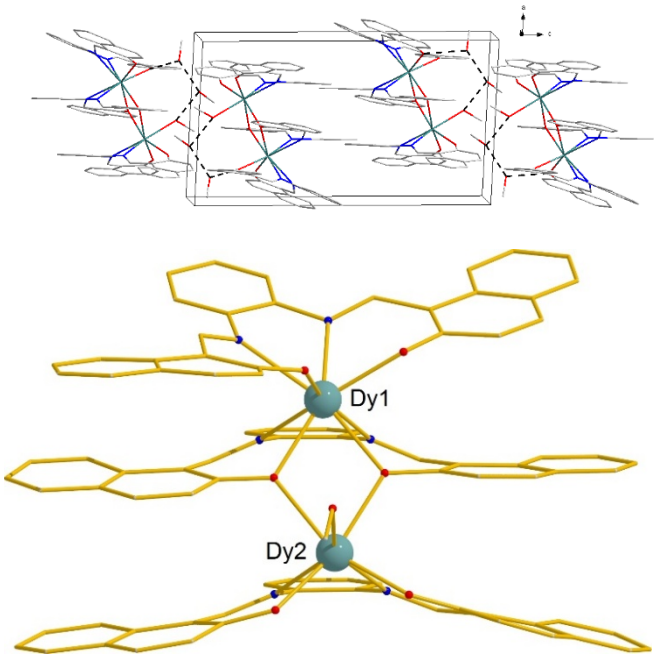

Figure 8 Crystal packing for **7**, showing the inter-molecular H-bonds (dashed lines).

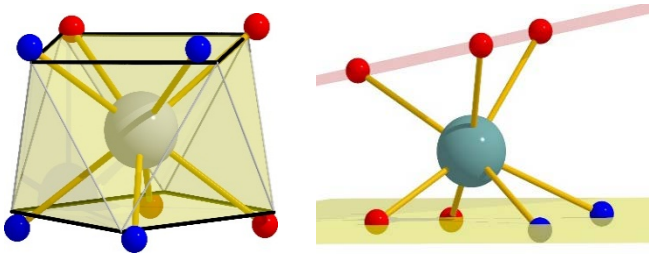

Magnetochemistry

Dc Magnetization and Magnetocaloric Studies

Direct current magnetic susceptibility studies were performed on polycrystalline samples of **1**-**8** in the 2 – 300 K range under an applied field of 0.1 T, and the results are plotted as the $\chi_M T$ product *vs*. *T* in Figure 9. Isothermal magnetization curves, *M* vs. *H*, for **1**-**8** for *H* up to 5 T are reported in Figures S4-S11 of the Supporting Information.

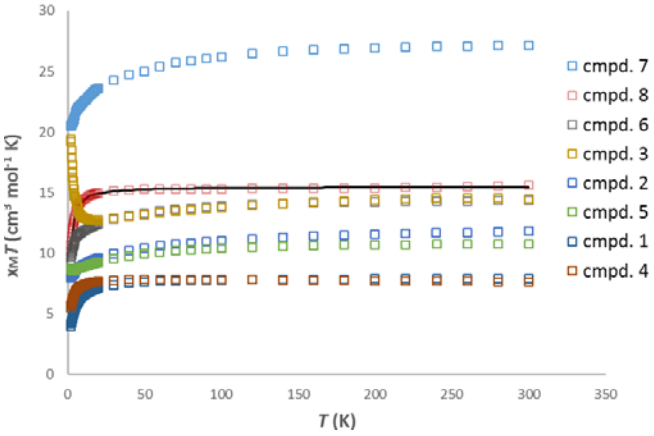

Figure 9 $X_M T$ *vs. T* plot for compounds **1** ([Gd/OH]*n*), **2** ([Tb/OH]*n*), **3** ([Dy/OH]*n*), **4** (Gd/N_3)*n*], **5** ([Tb/N_3]*n*), **6** ([Dy/N_3]*n*), **7** ([Dy_2]) and **8** ([Gd_2]), under an applied *dc* field of 1000 G. The solid line represents a fit of the magnetic susceptibility data for **8** (see text for details).

From a quick look at the susceptibility in Fig. 9, we observe two main trends present: i) compounds **1**, **2, 4, 5, 6, 7** and **8** display decreasing $\chi_M T$ product upon cooling, and ii) compound **3** displays a decreasing $\chi_M T$ product upon cooling, followed by a sudden increase at low temperatures. Another noteworthy observation, is the fact that the substitution of the bridging hydroxide groups by *end*-on azide ligands, does not seem to have a clear impact on the magnetic behaviour of the compounds, besides the case of the Dy^{III} analogue **3** which surprisingly enough switches from "ferromagnetic" (for the hydroxide analogue) to "antiferromagnetic" (for the azide version); obviously, the small geometric changes between the two kinds of bridges of **3** and **6** switch the sign of the magnetic exchange interaction.

More specifically, for the Gd analogues **1** and **4**, the room temperature $\chi_M T$ values of 7.92 $cm^3mol^{-1}K$ and 7.64 $cm^3mol^{-1}K$, respectively, are very close to the theoretical value of 7.87 $cm^3 mol^{-1}$ K expected for a Gd^{III} ion (g = 2.00). Upon cooling the $\chi_M T$ values remain constant until ~40 K, before they decrease to their minimum value of 4.00 cm^3 mol^{-1} K and 5.49 cm^3 $mol^{-1}K$, for **1** and **4**, respectively. For **2** and **5** (Tb analogues), the room-temperature $\chi_M T$ values are 11.84 $cm^3mol^{-1}K$ and 10.76 $cm^3mol^{-1}K$, respectively, very close to the theoretical $\chi_M T$ value of 11.80 expected for a Tb^{III} ion (g_J = 1.5). Upon cooling, the $\chi_M T$ values remain practically unchanged until ~100 K, below which they gradually decrease to reach the minimum value of 7.99 $cm^3mol^{-1}K$ for **2** and 8.68 $cm^3mol^{-1}K$ for **5**. Concerning the two Dy^{III} polymers, **3** and **6**, the room-temperature values of 14.57 $cm^3mol^{-1}K$ and 14.35 $cm^3mol^{-1}K$, respectively, are very close to the theoretical value corresponding to one Dy^{III} ion (g_J = 1.33) of 14.16 $cm^3mol^{-1}K$. Upon cooling the $\chi_M T$ product for **3** slightly decreases until ~10 K to the value of 12.68 $cm^3mol^{-1}K$, before

rapidly increasing to its maximum value of 19.41 $cm^3mol^{-1}K$ at 2.0 K. On the other hand, the $\chi_M T$ product for **6** slightly decrease to the value of 12.74 $cm^3mol^{-1}K$ at ~30 K, before it further decreases to its minimum value of 9.30 $cm^3mol^{-1}K$ at 2.0 K. Finally, regarding the two dimer complexes: i) for complex **7** ([Dy_2]) the room-temperature $\chi_M T$ value of 27.13 $cm^3mol^{-1}K$, very close to the theoretical value of 28.33 $cm^3mol^{-1}K$ expected for two non-interacting Dy^{III} ions, slightly decreases to 26.19 $cm^3mol^{-1}K$ at ~100 K, before reaching the minimum value of 20.45 $cm^3mol^{-1}K$ at 2.0 K; ii) for the Gd analogue **8**, the room-temperature value of 15.59 $cm^3mol^{-1}K$ very close to the theoretical value of 15.74 $cm^3mol^{-1}K$ for two non-interacting Gd^{III} centers, remains constant until ~40 K, before it reaches the minimum value of 9.77 $cm^3mol^{-1}K$ at 2.0 K.

For **1**, **4** and **8** the shape of the $\chi_M T$ product *vs*. *T* plot allows us to safely assume antiferromagnetic interactions between neighboring Gd pairs, while for **2**, **3**, **5**, **6** and **7** the curvature of the $\chi_M T$ product *vs*. *T* plot is not a good indicator of either ferro- or anti-ferromagnetic interactions, due to the depopulation of the m_J sublevels of the lanthanide centers (usually termed as *Stark* sublevels). In order to confirm the dominant interactions within **1**, **4** and **8**, we performed a Curie-Weiss analysis of the magnetic susceptibility data yielding θ values of -2.23 K, -0.71 K and -0.890 K, for **1**, **4** and **8**, respectively.

Given that in the Gd analogues **1** and **4**, all Gd···Gd intrachain distances are the same (3.955(1) Å in **1** and 3.974(1) Å in **4**) we managed to fit the magnetic susceptibility data, assuming a wheel-like structure[15] containing six Gd^{III} centers with one magnetic interaction between neighboring centers, *J* (Figure 10). Using the program PHI[16] and employing the Hamiltonian in eqn. (4)

$$\hat{H} = -2J\,(\hat{S}_1\cdot\hat{S}_2 + \hat{S}_2\cdot\hat{S}_3 + \hat{S}_3\cdot\hat{S}_4 + \hat{S}_4\cdot\hat{S}_5 + \hat{S}_5\cdot\hat{S}_6 + \hat{S}_6\cdot\hat{S}_1) \quad (4)$$

afforded the parameters J = -0.05 cm^{-1} and g = 2.00 for **1**, and J = -0.02 cm^{-1} and g = 2.00 for **4**. Such weak interactions are well expected for Gd pairs due to the inner nature of the 4*f* electrons, and are in excellent agreement with previously reported values.[17]

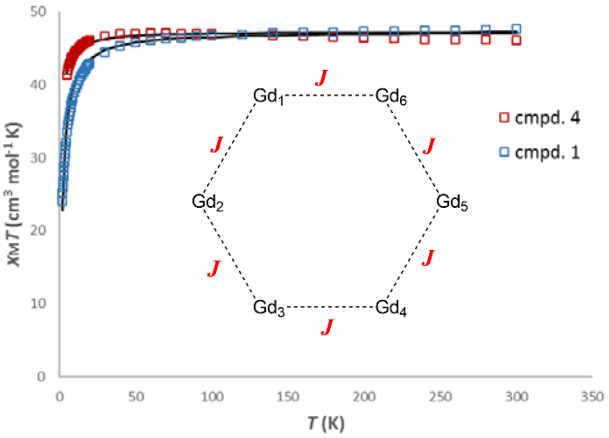

Figure 10 Magnetic susceptibility data for **1** (blue squares) and **4** (red squares) multiplied by six and best fit (solid lines) obtained by the using a wheel-like [Gd_6] interaction scheme (inset).

For the dimer cluster **8**, we were able to successfully fit the magnetic susceptibility data assuming one magnetic interaction, *J*, between the two centers. Using the Hamiltonian eqn. (5) and the mathematical formula in eqn. (6):[18]

$$\hat{H} = -J\,(\hat{S}_1\cdot\hat{S}_2) \quad (5)$$

$$x_M = (2N_A\beta^2 g^2)/(kT)\,F(J) \quad (6)$$

where

$$F(J) = (e^{2x} + 5e^{6x} + 14e^{12x} + 30e^{20x} + 55e^{30x} + 91e^{42x} + 140e^{56x})/(1 + 3e^{2x} + 5e^{6x} + 7e^{12x} + 9e^{20x} + 11e^{30x} + 13e^{42x} + 15e^{56x})$$

with $\chi = J/kT$, where N_A is the Avogadro constant, β the Bohr magneton, g the Landé -factor, k the Boltzmann constant and T the absolute temperature. The best parameters obtained were J = -0.04 cm^{-1} and g = 1.99, in very good agreement with previously reported systems.[18]

For compound **3**, {Dy/OH/polymer}, we used the non-critical scaling theory in order to study the ferromagnetic-like behaviour, using the sum of the two exponential functions in eqn. (7):[19]

$$\chi T = C_1\exp(E_1/T) + C_2\exp(E_2/T) \quad (7)$$

in which the sum of $C_1 + C_2$ is the high-temperature extrapolated *Curie* constant, E_1 represents a ferromagnetic contribution dominant at low temperatures and E_2 denotes a high temperature crystal-field effect. Fitting of the magnetic susceptibility data in the 2-300 K temperature range (Figure 11) yields C_1 = 11.44 $cm^3mol^{-1}K$, C_2 = 3.16 $cm^3mol^{-1}K$, E_1 = 1.08 K and E_2 = -44.32 K, thus indicating ferromagnetic intra-chain interactions.[20] That was further supported upon subtraction of the second term from the magnetic susceptibility data, resulting in a net ferromagnetic contribution, $\chi_F T = \chi T - C_2\exp(E_2/T)$.[19, 20] Despite the fact that many 1D Dy^{III} containing coordination

polymers have been reported to date,[21] only a handful have been found to display ferromagnetic intra-chain interactions.[20,22]

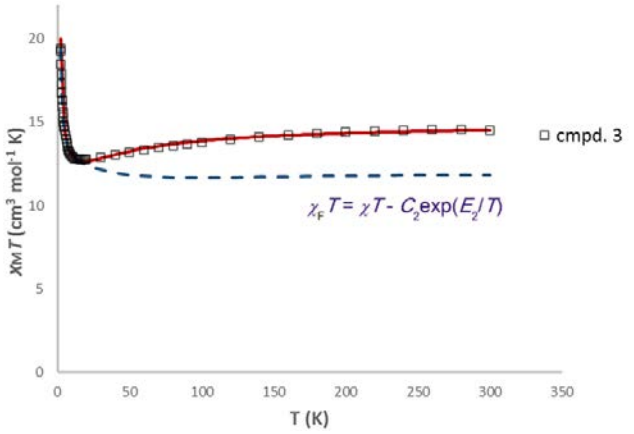

Figure 11 Fit of the magnetic susceptibility data for **3** (black squares) using the scaling theory (red line). The blue dashed line represents the resulting net ferromagnetic contribution, $\chi_F T = \chi T - C_2 \exp(E_2/T)$.

Next, we study the magnetocaloric properties of the Gd analogues, namely **1**, **4** and **8**. We derive the change of the magnetic entropy, ΔS_m, which follows from the change of the applied magnetic field, ΔB, by applying the Maxwell equation:

$$\Delta S_m(T, \Delta B) = \int [\partial M(T, B)/\partial T]_B dB, \quad (8)$$

to the magnetization data, M, (Figures S4, S7 and S11). To facilitate the comparison between the results inferred from each compound, the $\Delta S_m(T, \Delta B)$ data are reported per molar unit (right axis in Figure 12), in addition to per mass unit (left axis). For the dimer cluster **8**, the molar data are normalized also per Gd atom to further expedite the comparison. For any investigated ΔB and experimentally accessed T range, $-\Delta S_m(T, \Delta B)$ of each compound increases on lowering the temperature. Note that $-\Delta S_m(T, \Delta B)$ cannot exceed the maximum entropy value per mole Gd involved, which corresponds to $R\ln(2S_{Gd}+1) = 2.08\ R$, where $S_{Gd} = 7/2$. For the maximum applied field change (ΔB = 5 T) and T = 3 K, $-\Delta S_m$ reaches 21.8 Jkg^{-1}K^{-1} = 1.4 R for **1**, 23.0 Jkg^{-1}K^{-1} = 1.6 R for **4**, 16.0 Jkg^{-1}K^{-1} = 1.6 R (per mole Gd) for **8**. These values are somewhat smaller than the ones found for the same ΔB and T in other Gd-based compounds exhibiting 1D polymeric or dimeric structures.[6d,23] In terms of molar Gd units, **4** and **8** provide almost identical $-\Delta S_m(T, \Delta B)$ curves (Figure 12). For **1**, we observe a smaller MCE, which has to be ascribed to the presence of relatively stronger antiferromagnetic interactions, as already evidenced from magnetic measurements.

As well known, antiferromagnetic interactions are the least favorable for observing a large MCE.[7] In terms of mass units, the two polymers **1** and **4** show a much larger MCE than the dimer cluster **8**. This is chiefly due to the difference in the Gd density, *i.e.*, the metal:non-metal mass ratio.[6d,6e,23] Despite **8** having two Gd atoms per formula unit that contribute to the MCE and **1** and **4** only one, both polymers have a nearly three-times lighter molecular mass than the dimer. In terms of applications, this means that to obtain the same cooling power ($= -\int \Delta S_m dT$) we should use *ca.* 40-50 % more material for **8** than **1** or **4**.

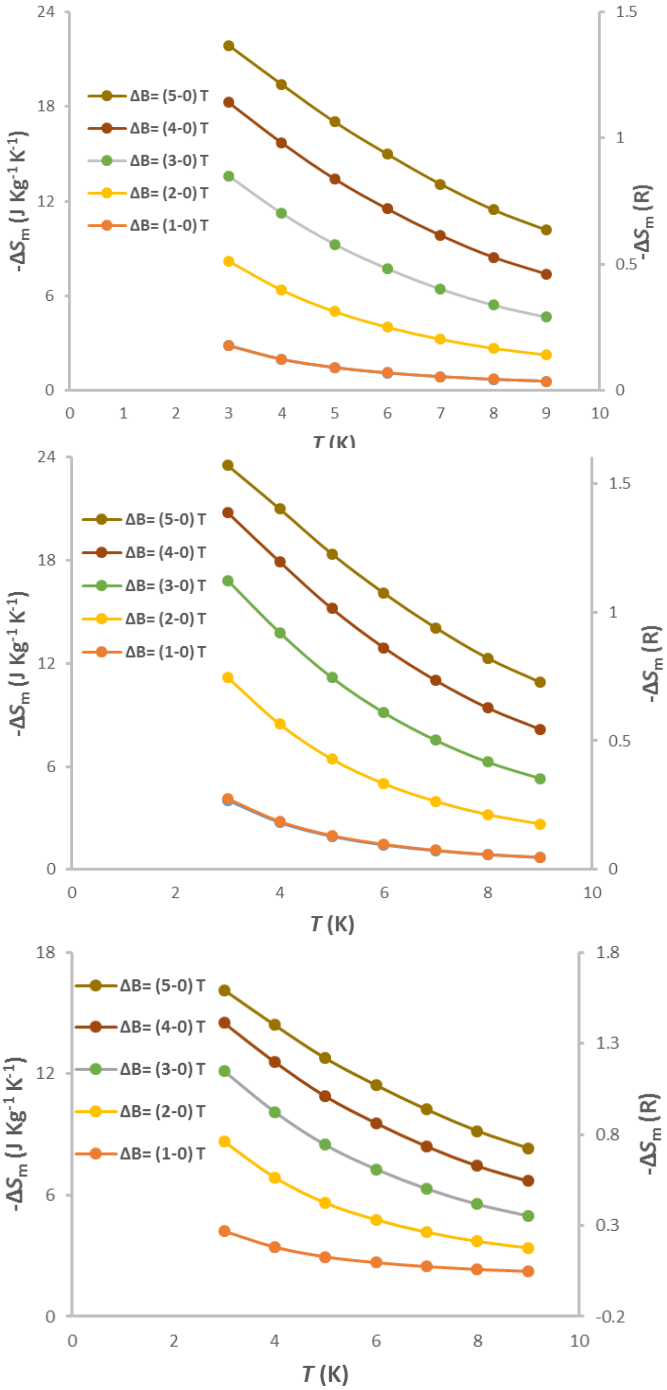

Figure 12 From top to bottom, magnetic entropy change for ΔB = (1 – 0), (2 – 0), (3 – 0), (4 – 0) and (5 – 0) T, as calculated from magnetization data for **1**, **4** and **8**, respectively. Lines are guides for the eyes. Values of the magnetic entropy change are expressed per mass unit (left axis) and per mole Gd unit (right axis).

Ac Magnetic Susceptibility Studies

Alternating current magnetic susceptibility studies were performed on samples of **2**, **3**, **5**, **6** and **7**, in the 1.8 – 20 K range under zero applied *dc* field and 4.0 G *ac* field oscillating at 7 – 1285 Hz range, as a means of investigating possible magnetic relaxation phenomena. The two terbium analogues, **2** and **5**, showed no frequency in-phase magnetic susceptibility dependence, as well as no out-phase-signals, suggesting the absence of magnetic relaxation in these species. On the contrary, all dysprosium compounds display interesting *ac* magnetic behaviour; for **3**, the temperature dependence of the in-phase, χ_M', and out-of-phase, χ_M'', magnetic susceptibility

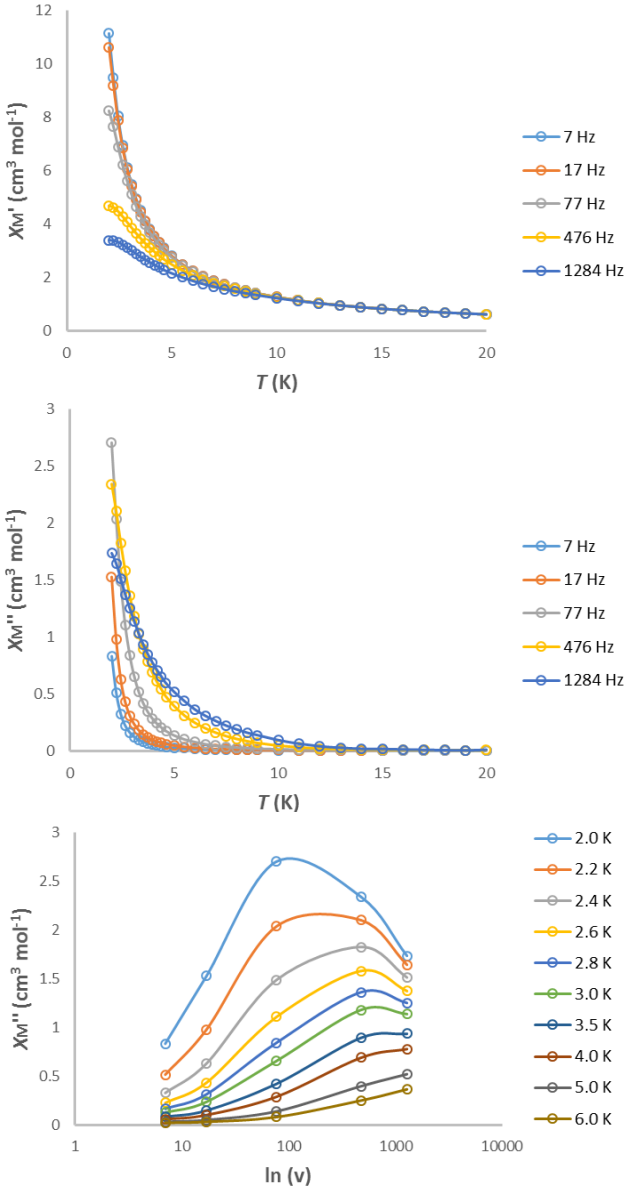

Figure 13 Plot of the in-phase χ_M' (top) and out-of-phase χ_M'' signals (center) for **3** in ac susceptibility studies vs. *T* in a 4.0 G oscillating field at the indicated frequencies. Plot of the out-of-phase χ_M'' signals *vs.* ln(*ν*) at the indicated temperatures (bottom). Lines are guides for the eyes.

under zero static *dc* field is shown in Figure 13 (top and center), together with the frequency dependence of the out-of-phase magnetic susceptibility (Figure 13, bottom). As it can be seen, both the in-phase and the out-of-phase magnetic susceptibility signals present temperature dependence below ~10 K, and in combination with the frequency dependence of the out-of-phase signals slow magnetic relaxation in these species is suggested. Unfortunately, no fully formed out-of-phase signals (peaks) are observed, and thus no further analysis was possible. Similarly, this is the case for **6**, since temperature dependence of both the in-phase and out-of-phase signals is observed at temperatures < 15 K (Figure 14), but again no characteristic maxima in the out-of-phase signals are observed. Yet, one significant observation is that this dependence now occurs at elevated temperature than the corresponding one for compound **3** (15 K for **6** *vs.* 10 K for **3**), thus indicating the impact of substituting the bridging methoxide groups in **3** with azide groups in **6**, since it is well established that both the coordination sphere and the environment of the 4*f* center plays an important role in magnetic relaxation phenomena.[24]

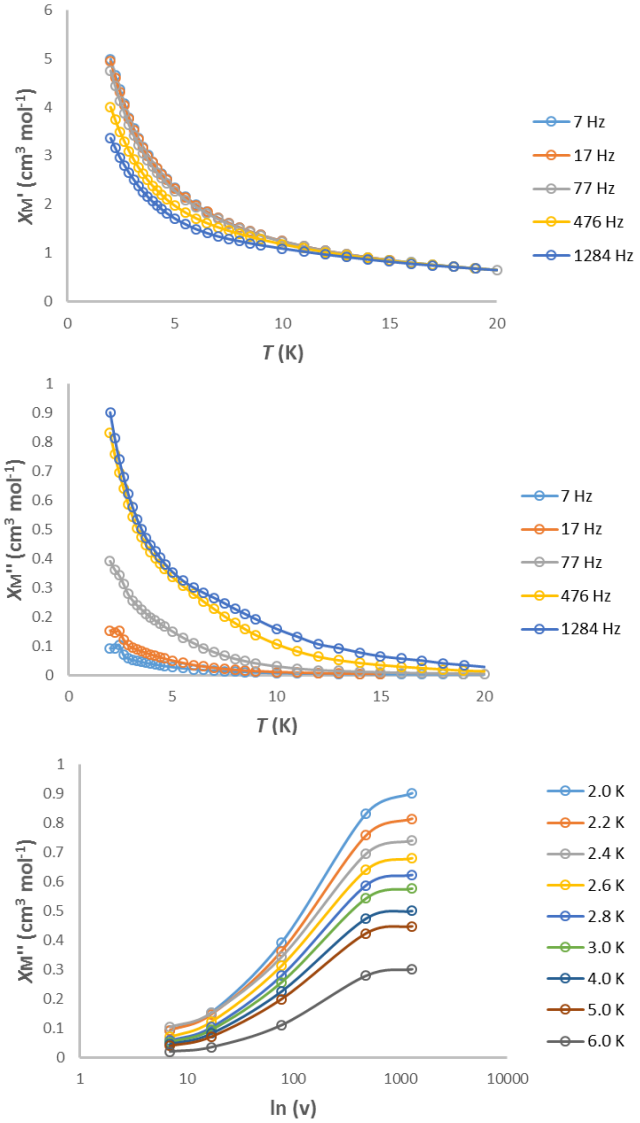

Figure 14 Plot of the in-phase χ_M' (top) and out-of-phase χ_M'' signals (center) for **6** in ac susceptibility studies vs. *T* in a 4.0 G oscillating field at the indicated frequencies. Plot of the out-of-phase χ_M'' signals *vs.* ln(*ν*) at the indicated temperatures (bottom). Lines are guides for the eyes.

Given the absence of high symmetry for the dysprosium centres in **6**, we were able to utilize the electrostatic model recently reported by Chilton et al., which performs electrostatic energy minimization for the prediction of the ground-state magnetic anisotropy axis.[25] Following this approach and program MAGELLAN, the ground state magnetic anisotropy axes for the Dy center in **6** was found to be tilted towards the O2 atoms (O2A and O2B) belonging to the alkoxide groups of the salen-type ligand connected on the lanthanide center (Fig. 15). Despite the fact that there is only one type of Dy centers present in **6**, there are two orientations of the magnetic anisotropy axes due to the zig-zag conformation of the chain, with the two "kinds" of axis tilted by ~110° with respect to each other.

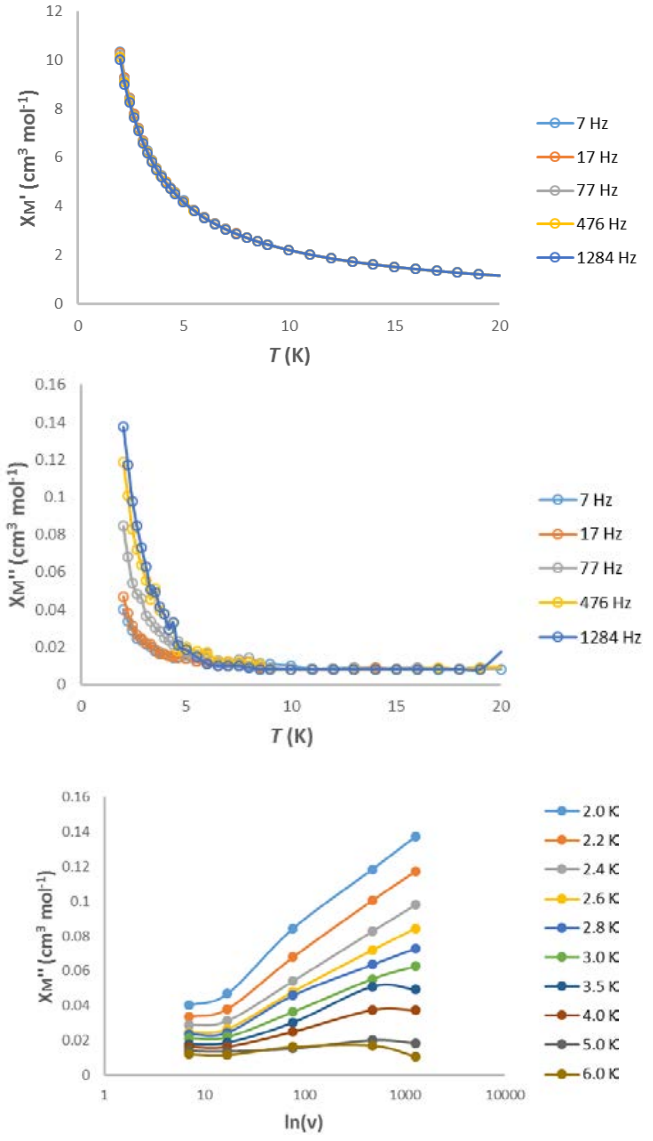

Figure 15 (Top) Ground state magnetic anisotropy axes (blue and red bold lines) for the Dy centers present in **6** looking down *c* axis; (bottom) the relative orientation of the magnetic anisotropy axes of the Dy^{III} ions in **6** looking down the polymer propagation direction, axis *b*. Lines are guides for the eyes.

For the dimer complex $[Dy_2(L')_3(MeOH)]\cdot 2MeOH$ (**7**·2MeOH), a similar behaviour is observed; temperature dependent in-phase and out-of-phase signals are observed at temperatures < 10 K (Figure 16), but again no fully-formed out-of-phase peaks are observed. Given the asymmetric nature of the dimeric complex, two magnetic anisotropy axes were found (Fig. 17);[25] for Dy1 the axes are tilted towards O21 (terminal alkoxide), while for Dy2 is tilted towards O2F (bridging alkoxide) and O2A (terminal alkoxide).

A thorough CCDC search revealed over one hundred examples of dimeric, $[Dy_2]$ complexes reported to date, with the vast majority being symmetrical,[24e,26] while only few are non-symmetrical regarding the coordination sphere/environment of the metallic centres.[3g,14b, 27]

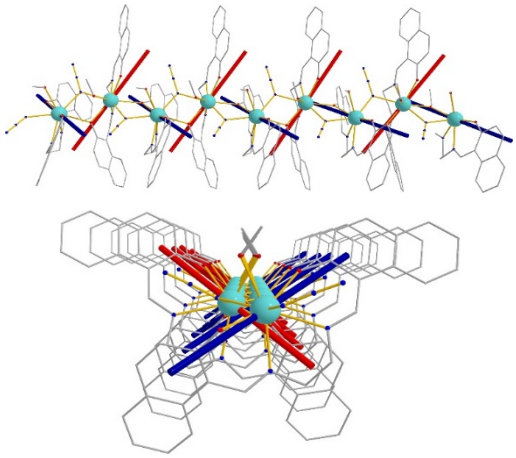

Figure 16 Plot of the in-phase χ_M' (top) and out-of-phase χ_M'' signals (center) for **7**, $[Dy_2]$, in ac susceptibility studies vs. *T* in a 4.0 G oscillating field at the indicated frequencies. Plot of the out-of-phase χ_M'' signals *vs.* ln(*v*) at the indicated temperatures (bottom).

Please do not adjust margins

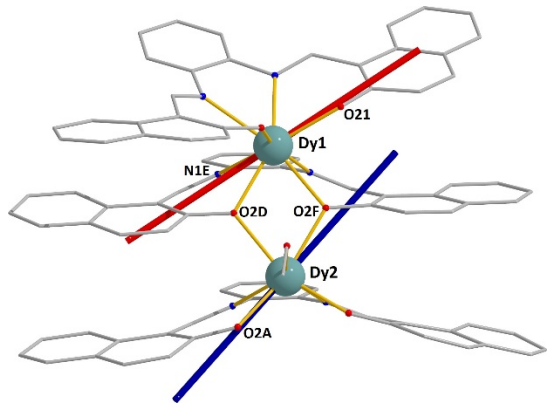

Figure 17 Ground state magnetic anisotropy axes (blue and red bold lines) for the Dy centers present in the dimeric complex **7**.

Conclusions

In conclusion, we have reported our results towards the synthesis of related lanthanide species; we were able to isolate and characterize two families of related 1-D coordination polymers, and their "analogous" discrete dinuclear building units upon employment of suitable "simple" chelate and bridging ligands. For all Dy analogues, the study of their magnetic properties revealed magnetic relaxation phenomena, while the magnetocaloric properties of all three Gd analogues were investigated.

Acknowledgements

CJM and ABC: "This research has been co-financed by the European Union (European Social Fund – ESF) and Greek national funds through the Operational Program "Education and Lifelong Learning" of the National Strategic Reference Framework (NSRF) - Research Funding Program: THALES. Investing in knowledge society through the European Social Fund". GL and ME thank Spanish MINECO (MAT2015-68204-R).

Notes and references

‡ Footnotes relating to the main text should appear here. These might include comments relevant to but not central to the matter under discussion, limited experimental and spectral data, and crystallographic data.

§

1 See for example: (a) O. Kahn, *Molecular Magnetism*, New York, Wiley-VCH, 1993; A. T. Casey and S. Mitra, *Theory and Applications of Molecular* Paramagnetism, New York, Interscience, 1976; (b) A. Abragam and B. Bleany, Electron Paramagnetic Resonance of Transition Ions, Dover Publications, Inc., New York, 1986.

2 N. Ishikawa, M. Sugita, T. Ishikawa, S. Koshihara and Y. Kaizu, *J. Am. Chem. Soc.*, 2003, **125**, 8694.

3 Representative references and refs. therein: (a) R. Sessoli and A. K. Powell, *Coord. Chem. Rev.*, 2009, ***253***, 2328; (b) D. N. Woodruff, R. E. P. Winpenny and R. A. Layfield, *Chem. Rev.*, 2013, **113**, 5110; (c) J. D. Rinehart and J. R. Long, *Chem. Sci.*, 2011, **2**, 2078; (d) Y. -N. Guo, G. -F. Xu, Y. Guo and J. Tang, *Dalton Trans.*, 2011, **40**, 9953; (e) P. Zhang, Y.-N. Guo and J. Tang, *Coord. Chem. Rev.*, 2013, **257**, 1728; (f) Y.-N. Guo, G.-F. Xu, P. Gamez, L. Zhao, S.-Y. Lin, R. Deng, J. Tang and H.-J. Zhang, *J. Am. Chem. Soc.*, 2010, **132**, 8538; (g) Y.-N. Guo, G.-F. Xu, W. Wernsdorfer, L. Ungur, Y. Guo, J. Tang, H.-J. Zhang, L. F. Chibotaru and A. K. Powell, *J. Am. Chem. Soc.*, 2011, **133**, 11948.

4 M. Gonidec, R. Biagi, V. Corradini, F. Moro, V. De. Renzi, U. Pennino, D. Summa, L. Muccioli, C. Zannoni, D. B. Amabilino and J. Veciana, *J. Am. Chem. Soc.*, 2011, **133**, 6603.

5 R. J. Blagg, L. Ungur, F. Tuna, J. Speak, P. Comar, D. Collison, W. Wernsdorfer, E. J. L. McInnes, L. F. Chibotaru and R. E. P. Winpenny, *Nat. Chem.*, 2013, **5**, 673.

6 (a) For a recent overview, see, for example, J. W. Sharples and D. Collison, *Polyhedron*, 2013, **54**, 91, and references therein; (b) G. Karotsis, M. Evangelisti, S. J. Dalgarno and E. K. Brechin, *Angew. Chem. Int.-Ed.*, 2009, **48**, 9928; (c) J. W. Sharples, Y.-Z. Zheng, F. Tuna, E. J. L. McInnes and D. Collison, *Chem. Commun.*, 2011, **47**, 7650; (d) M. Evangelisti, O. Roubeau, E. Palacios, A. Camón, T. N. Hooper, E. K. Brechin and J. J. Alonso, *Angew. Chem. Int.-Ed.*, 2011, **50**, 6606; (e) G. Lorusso, M. Jenkins, P. González-Monje, A. Arauzo, J. Sesé, D. Ruiz-Molina, O. Roubeau and M. Evangelisti, *Adv. Mater.*, 2013, **25**, 2984; (f) G. Lorusso, J. W. Sharples, E. Palacios, O. Roubeau, E. K. Brechin, R. Sessoli, A. Rossin, F. Tuna, E. J. L. McInnes, D. Collison and M. Evangelisti, *Adv. Mater.*, 2013, **25**, 4653; (g) J. W. Sharples, D. Collison, E. J. L. McInnes, J. Schnack, E. Palacios and M. Evangelisti, *Nat. Commun.*, 2014, **5**, 5321; (h) G. Lorusso, O. Roubeau and M. Evangelisti, *Angew. Chem. Int.-Ed.*, 2016, **55**, 3360.

7 (a) M. Evangelisti, E. K. Brechin, *Dalton Trans.*, 2010, **39**, 4672; (b) M. Evangelisti, Molecule-Based Magnetic Coolers: Measurement, Design and Application, in *Molecular Magnets: Physics and Applications*, ed. J. Bartolomé, F. Luis and J. F. Fernández, Springer, Verlag Berlin Heidelberg, 2014, pp. 365–387.

8 M. Evangelisti, A. Candini, M. Affronte, E. Pasca, L. J. de Jongh, R. T. W. Scott, E. K. Brechin, *Phys. Rev. B* **2009**, *79*, 104414.

9 R. E. P. Winpenny, *Dalton Trans.*, **2002**, *1*. PAG??????

10 G. M. Sheldrick, *Acta Crystallogr.* **2008**, *A64*, 112–122.

11 Representative references and refs. therein: (a) J. Ribas, A. Escuer, M. Monfort, R. Vicente, R. Cortes, L. Lezama and T. Rojo, *Coord. Chem. Rev.*, 1999, **193**, 1027; (b) A. Escuer and G. Aromi, *Eur. J. Inorg. Chem.*, 2006, 4721; (c) Y. -F. Zeng, X. Hu, F. -C. Liu and X. -H. Bu, *Chem. Soc. Rev.*, 2009, **38**, 469; (d) A. Escuera, J. Esteban, S. P. Perlepes and T. C. Stamatatos, *Coord. Chem. Rev.*, 2014, **275**, 87; (e) N. M. Randell, M. U. Anwar, M. W. Drover, L. N. Dawe and L. K. Thompson, *Inorg. Chem.*, 2013, **52**, 6731; (f) M. U. Anwar, L. K. Thompson, L. N. Dawe, F. Habib and M. Murugesu, *Chem. Commun.*, 2012, **48**, 4576.

12 R. A. Coxall, S. G. Harris, D. K. Henderson, S. Parsons, P. A.Tasker and R. E. P. Winpenny, *J. Chem. Soc, Dalton Trans.*, 2000, 2349.

13 M. Llunell, D. Casanova, J. Girera, P. Alemany and S. Alvarez, SHAPE, version 2.0, Barcelona, Spain 2010.

14 (a) H.-J. Kim, D. Whang, K. Kim and Y. Do, *Inorg. Chem.*, 1993, **32**, 360; (b) F. Gao, Y.-Y. Li, C.-M. Liu, Y.-Z. Lia and J.-L. Zuo, *Dalton Trans.*, 2013, **42**, 11043; (c) G. S. Girolami, S. N. Milam and K. S. Suslick, *Inorg. Chem.*, 1987, **26**, 343.

15 A. Escuer, M. S. El Fallah, R. Vicente, N. Sanz, M. Font-Bardia, X. Solans and F. A. Mautner, *Dalton*, 2004, 1867.

16 N. F. Chilton, R. P. Anderson, L. D. Turner, A. Soncini and K. S. Murray, *J. Comput. Chem.*, 2013, **34**, 1164.

17 See for example: (a) A. Rohde and W. Urland, *Dalton Trans.*, 2006, 2974; (b) A. Rohde, S. T. Hatscher and W. Urland, *J. Alloys Compd.*, 2004, **374**, 137; (c) A. Rohde and W. Urland, *J. Alloys Compd.*, 2006, **408-412**, 618; (d) A. Rohde and W. Urland, *Z. Anorg. Allg. Chem.*, 2005, **631**, 417; (e) A. Rohde and W. Urland, *Z. Anorg. Allg. Chem.*, 2004, **630**, 2434; (f) S. T.

Please do not adjust margins

Please do not adjust margins

Hatscher and W. Urland, *Angew. Chem., Int. Ed.*, 2003, **42**, 2862; (g) M. Hernández-Molina, C. Ruiz-Pérez, T. López, F. Lloret and M. Julve, *Inorg. Chem.*, 2003, **42**, 5456; (h) H. Hou, G. Li, L. Li, Y. Zhu, X. Meng and Y. Fan, *Inorg. Chem*., 2003, **42**, 428; (i) A. W.-H. Lam, W.-T. Wong, S. Gao, G. Wen and X.-X. Zhang, *Eur. J. Inorg. Chem.*, 2003, 149; (j) D. John and W. Urland, *Eur. J. Inorg. Chem*., 2005, 4489.

18 A. Panagiotopoulos, T. F. Zafiropoulos, S. P. Perlepes, E. Bakalbassis, I. Masson-Ramade, O. Kahn, A. Terzis and C. P. Raptopoulou, *Inorg. Chem.*, 1995, **34**, 4918.

19 J. Souletie, P. Rabu, M. Drillon, *Phys. Rev. B,* 2005, **72**, 214427; M. Drillon, P. Panissod, P. Rabu, J. Souletie, V. Ksenofontov and P. Gütlich, *Phys. Rev. B,* 2002, **65**, 104404.

20 See for example: Y.-Z. Zheng, Y. Lan, W. Wernsdorfer, C. E. Anson and A. K. Powell, *Chem. Eur. J.*, 2009, **15**, 12566.

21 Representative references and refs. therein: (a) J. M. Tian, B. Li, X. Y. Zhang, X. L. Li, X. L. Li and J. P. Zhang, *Dalton Trans*., 2013, **42**, 8504; (b) Y. Zhu, F. Luo, Y. M. Song, H. X. Huang, G. M. Sun, X. Z. Tian, Z. Z. Yuan, Z. W. Liao, M. B. Luo, S. J. Liu, W. Y. Xu and X. F. Feng, *Dalton Trans*., 2012, **41**, 6749; (c) D. Alexandropoulos, C. Li, C. P. Raptopoulou, V. Psycharis, W. Wernsdorfer, G. Christou and T. C. Stamatatos, *Curr. Inorg. Chem.*, 2013, **3**, 161; (d) F. Luo, Z. W. Liao, Y. M. Song, H. X. Huang, X. Z. Tian, G. M. Sun, Y. Zhu, Z. Z. Yuan, M. B. Luo, S. J. Liu, W. Y. Xu and X. F. Feng, *Dalton Trans*., 2011, **40**, 12651; (e) L. Bogani, C. Sangregorio, R. Sessoli and D. Gatteschi, *Angew. Chem., Int. Ed.*, 2005, **44**, 5817; (f) K. Bernot, L. Bogani, A. Caneschi, D. Gatteschi and R. Sessoli, *J. Am. Chem. Soc.*, 2006, **128**, 7947; (g) C.-B. Han, Y.-L. Wang, Y.-L. Li, C.-M. Liu and Q.-Y. Liu, *Inorg. Chem. Commun*., 2015, **58**, 91; (h) T. Han, J.-D. Leng, Y.-S. Ding, Y. Wang, Z. Zhenga and Y.-Z. Zheng, *Dalton Trans*., 2015, **44**, 13480; (i) J. Jung, F. L. Natur, O. Cador, F. Pointillart, G. Calvez, C. Daiguebonne, O. Guillou, T. Guizouarn, B. L. Guennic and K. Bernot, *Chem. Commun*., 2014, **50**, 13346; (j) Q. Chen, Y. S. Meng, Y. Q. Zhang, S. D. Jiang, H. L. Sun and S. Gao, *Chem. Commun*., 2014, **50**, 10434.

22 (a) Y. Wang, T. W. Wang, Y. Song and X. Z. You, *Inorg. Chem*., 2010, **49**, 969; (b) Y. L. Hou, G. Xiong, B. Shen, B. Zhao, Z. Chen and J. Z. Cui, *Dalton Trans*., 2013, **42**, 3587; (c) P. I. Girginova, L. C. J. Pereira, J. T. Coutinho, I. C. Santos and M. Almeida, *Dalton Trans*., 2014, **43**, 1897; (d) L. Jia, Q. Chen, Y. S. Meng, H. L. Sun and S. Gao, *Chem. Commun*., 2014, **50**, 6052; (e) W.-H. Zhu, Y. Zhang, Z. Guo, S. Wang, J. Wang, Y.-L. Huang, L. Liu, Y.-Q. Fan, F. Cao and S.-W. Xiang, *RSC Adv.*, 2014, **4**, 49934; (f) Y. D. Luo, G. M. Sun, D. M. Li and F. Luo, *Inorg. Chem. Commun*., 2011, **14**, 778.

23 (a) G. Lorusso, M. A. Palacios, G. S. Nichol, E. K. Brechin, O. Roubeau and M. Evangelisti, *Chem. Commun*., 2012, **48**, 7592; (b) F.-S. Guo, J.-D. Leng, J.-L. Liu, Z.-S. Meng and M.-L. Tong, *Inorg. Chem.*, 2012, **51**, 405.

24 See for example: (a) Y. Bi, Y.-N. Guo, L. Zhao, Y. Guo, S.-Y. Lin, S.-D. Jiang, J. Tang, B.-W. Wang and S. Gao, *Chem. Eur. J*., 2011, **17**, 12476; (b) X.-L. Mei, Y. Ma, L.-C. Li and D.-Z. Liao, *Dalton Trans*., 2012, **41**, 505; (c) G. J. Chen, Y.-N. Guo, J. L. Tian, J. Tang, W. Gu, X. Liu, S. P. Yan, P. Cheng and D. Z. Liao, *Chem. Eur. J*., 2012, **18**, 2484; (d) E. Bartolomé, J. Bartolomé, S. Melnic, D. Prodius, S. Shova, A. Arauzo, J. Luzón, F. Luis and C. Turtac, *Dalton Trans*., 2013, **42**, 10153; (e) J. Long, F.Habib, P. H. Lin, I. Korobkov, G. Enright, L. Ungur, W. Wernsdorfer, L.F. Chibotaru and M. Murugesu, *J. Am. Chem. Soc*., 2011, **133**, 5319; (f) D. P. Li, T. W. Wang, C. H. Li, D. S. Liu, Y. Z. Li and X. Z. You, *Chem. Commun*. 2010, **46**, 2929; (g) W.-M. Wang, H.-X. Zhang, S.-Y. Wang, H.-Y. Shen, H.-L. Gao, J.-Z. Cui and B. Zhao, *Inorg. Chem.*, 2015, **54**, 10610.

25 N. F. Chilton, D. Collison, E. J. L. McInnes, R. E. P. Winpenny and A. Soncini, *Nat. Commun*., 2013, **4**, 2551.

26 Representative references: (a) F. Habib, P. H. Lin, J. Long, I. Korobkov, W. Wernsdorfer and M. Murugesu, *J. Am. Chem. Soc*., 2011, **133**, 8830; (b) F. Habib, G. Brunet, V. Vieru, I. Korobkov, L. F. Chibotaru and M. Murugesu, *J. Am. Chem. Soc.*, 2013, **135**, 13242; (c) P. Bag, C. K. Rastogi, S. Biswas, S. Sivakumar, V. Mereacre and V.Chandrasekhar, *Dalton Trans.,* 2015, **44**, 4328; (d) X.-F. Tan, X. Liu, J. Zhou, R. Zhao, Y. Xie and Q. Tang *J. Cluster Sci.,* 2015, **26**, 1503; (e) S. Xue, Y.-N. Guo, L. Ungur, J. Tang and L. F. Chibotaru, *Chem.-Eur. J.*, 2015, **21**, 14099; (f) X. Tan, X. Ji and J.-M. Zheng, *Inorg.Chem.Commun.,* 2015, **60**, 27; (g) F. Zhou, S. Zhang, Y. Zhao, C. Zhang, X. Cheng, L. Zheng, Y. Zhang and Y. Li, *Z. Anorg. Allg. Chem.,* 2009, **635**, 26; (h) P. Zheng, J. Hong, R. Liu, Z. Zhang, Z. Pang, L. Weng and X. Zhou, *Organometallics,* 2010, **29**, 1284; (i) M. S. Khiyalov, I. R. Amiraslanov, K. S. Mamedov and E. M. Movsumov, *Koord. Khim. (Russ.) (Coord. Chem.)*, 1981, **7**, 445; (j) Y. Inomata, T. Sunakawa and F. S. Howell, *J. Mol. Struct.,* 2003, **648**, 81; (k) J. Wang, S. Li, C. Zheng, J. A. Maguire, B. Sarkar, W. Kaim and N. S. Hosmane, *Organometallics,* 2003, **22**, 4334; (l) J.-B. Shen, J.-L. Liu and G.-L. Zhao, *Acta Crystallogr., Sect. E: Struct. Rep. Online,* 2011, **67**, m1320; (m) R. Chen, W. Tang, J. Liang, W. Jiang, Y. Zhang and D. Jia, *Dalton Trans.,* 2012, **41**, 12439; (n) F. Yang, Q. Zhou, G. Zeng, G. Li, L. Gao, Z. Shi and S. Feng, *Dalton Trans.,* 2014, **43**, 1238; (o) M. Ren, S.-S. Bao, N. Hoshino, T. Akutagawa, B. Wang, Y.-C. Ding, S. Wei and L.-M. Zheng, *Chem.-Eur. J.,* 2013, **19**, 9619; (p) Y.-Y. Zhang, N. Ren, S.-L. Xu, J.-J. Zhang and D.-H. Zhang, *J. Mol. Struct.,* 2015, **1081**, 413; (q) P.-H. Lin, T. J. Burchell, R. Clérac and M. Murugesu, *Angew. Chem., Int. Ed.,* 2008, **47**, 8848; (r) Y. Li, F.-K. Zheng, X. Liu, W.-Q. Zou, G.-C. Guo, C.-Z. Lu and J.-S. Huang, *Inorg. Chem.*, 2006, **45**, 6308.

27 (a) P.-H. Lin, W.-B. Sun, M.-F. Yu, G.-M. Li, P.-F. Yan and M. Murugesu, *Chem. Commun*., 2011, **47**, 10993; (b) M. Holynska, R .Clérac and M. Rouzieres, *Chem.-Eur. J.*, 2015, **21**, 13321; (c) D. Aguila, L. A. Barrios, V. Velasco, L. Arnedo, N. Aliaga-Alcalde, M. Menelaou, S. J. Teat, O. Roubeau, F. Luis and G. Aromi, *Chem.-Eur. J.,* 2013, **19**, 5881; (d) J.-P. Costes, F. Dahan and F. Nicodeme, *Inorg. Chem.,* 2003, **42**, 6556; (e) F. Gao, Y.-Y. Li, C.-M. Liu, Y.-Z. Li and J.-L. Zuo, *Dalton Trans.,* 2013*,* **42**, 11043; (f) K. Wang, S. Zeng, H. Wang, J. Dou and J. Jiang, *Inorg.Chem.Front.,* 2014, **1**, 167; (g) A.-J. Hutchings, F. Habib, P.-H. Lin, I. Korobkov and M. Murugesu, *Inorg.Chem. ,* 2014, **53**, 2102; (h) S. Anfang, K. Harms, F. Weller, O. Borgmeier, H. Lueken, H. Schilder and K. Dehnicke, *Z. Anorg. Allg. Chem.,* 1998, **624**, 159; (i) V. Patroniak, A. R. Stefankiewicz, J.-M. Lehn, M. Kubicki and M. Hoffmann, *Eur. J. Inorg. Chem.,* 2006, 144; (j) L. Zhang, Y. Ji, X. Xu, Z. Liu and J. Tang, *J. Lumin.,* 2012, **132,**1906; (k) E. M. Pineda, N. F. Chilton, R. Marx, M. Dorfel, D. O. Sells, P. Neugebauer, S.-D. Jiang, D. Collison, J. van Slageren, E. J. L. McInnes and R. E. P. Winpenny, *Nat. Commun.,* 2014, **5**, 5243; (l) L. Ma, J. Zhang, Z. Zhang, R. Cai, Z. Chen and X. Zhou, *Organometallics,* 2006, **25**, 4571; (m) Y.-N. Guo, X.-H. Chen, S. Xue and J. Tang, *Inorg. Chem.,* 2011, **50**, 9705; (n) J. Zhu, H.-F. Song, P.-F. Yan, G.-F. Hou and G.-M. Li, *CrystEngComm.,* 2013, **15**, 1747; (o) F. Gao, X.-M. Zhang, L. Cui, K. Deng, Q.-D. Zeng and J.-L. Zuo, *Scientific Reports,* 2014, **4**, 5928; (p) L. Zhang, P. Zhang, L. Zhao, S.-Y. Lin, S. Xue, J. Tang and Z. Liu, *Eur. J. Inorg. Chem.,* 2013, 1351; (q) H. Wang, C. Liu, T. Liu, S. Zeng, W. Cao, Q. Ma, C. Duan, J. Dou and J. Jiang, *Dalton Trans.,* 2013, **42**, 15355; (r) Y.-L. Chien, M.-W. Chang, Y.-C. Tsai, G.-H. Lee, W.-S. Sheu and E.-C. Yang, *Polyhedron,* 2015, **102**, 8.

Please do not adjust margins